PRIME - A synchrotron of a phased program for the Japan Hadron Project

Isao YAMANE, Toshikazu ADACHI, Takao KATO, Tadamichi KAWAKUBO,
Shigeshi NINOMIYA and Yoshiharu YANO
National Laboratory for High Energy Physics (KEK)
Oho-cho 1-1, Tsukuba-shi, Ibaraki-ken, 305 Japan

Chihiro OHMORI
Institute for Nuclear Study (INS), University of Tokyo
Midori-cho 3-2-1, Tanasi-shi, Tokyo-to, 188 Japan

abstract

A preliminary conceptual design of a high-intensity proton synchrotron proposed in a phased program for JHP has been carried out. This report presents results of design work on the main components of the synchrotron. The results of a computer simulation on beam painting are also given.

1. INTRODUCTION

JHP (Japan Hadron Project) was proposed in 1987, aiming to promote basic science covering a wide range of interdisciplinary fields. Recently an alternative to JHP, a phased program, has been proposed. The first phase is assigned to that part of JHP, pulse neutron scattering and pulsed muon science, that is considered to be most urgent. As is shown in Fig. 1, it comprises a 200 MeV-400 μA proton linac, a 1 GeV-200 μA synchrotron and two experimental halls. It was carefully considered that the remaining part of JHP should be easily extended in the following phases.

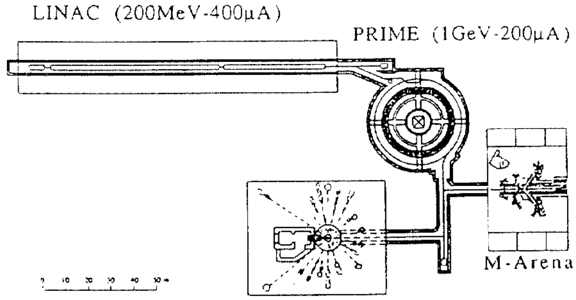

Fig. 1 Plan view of the proposed phased program for JHP

One of the main reasons why a system of a synchrotron and an injector linac has been adopted for the accelerator composition is that pulsed neutron scattering and pulsed muon science do not require a very small emittance for the primary proton beam. Upon choosing the energy of the linac, which is also the injection energy of the synchrotron, there were requirements from both sides of the linac and the synchrotron. In order to gain experience for the future extension, it was required from the linac side to include part of a high-β structure, which is effective in the energy region over 150 MeV. The requirement from the ring is that the injection energy should be low, as long as the necessary aperture of the magnets does not become too large due to space charge effects resulting from the high intensity.

2. SPECIFICATION OF THE PRIME RING

Table 1 Main beam parameters

Injected H^- beam		
Energy	200	MeV
Peak current	20	mA
Injection period	400	μsec
Width of micropulse	~ 190	nsec
Repetition rate	50	Hz
Average current	200	μA
Normalized emittance (ε_{xn}, ε_{yn})	2.6	π·mm·mrad
Energy spread	± 0.1	%
Beam just after injection		
Absolute emittance ε_x	150	π·mm·mrad
ε_y	125	π·mm·mrad
Revolution frequency	1.3	MHz
Number of beam bunches	2	
Bunch length	~ 190	nsec
Number of particles in a bunch	1.25×10^{13}	
Beam at the extraction		
Energy	1 (1.5)	GeV
Revolution frequency	2.3	MHz
Bunch length	~ 100	nsec
Absolute emittance Horizontal	42.9	π·mm·mrad
Vertical	35.7	π·mm·mrad
Momentum spread	±1	%

2.1 Main Beam Parameters

The main beam parameters are listed in Table 1. The H^- beam basically has the same specifications as that designed for the 1-GeV linac of JHP. As for the 1-GeV high intensity proton linac, a prototype of the low-energy part (< 10 MeV) has been constructed, and development is now being carried out.

The emittance of the beam just formed in the ring was determined so that the tune shift due to the space-charge force should be less than 0.25 in order to avoid integer and half-integer resonances. The tune shifts were estimated using the computer code SPACEX developed at RAL with optical parameters of the lattice described below. The code solved envelope equations including the term of the space charge force, under the condition that the charge distribution is of the Kapchinskij-Vladimirskij type. The formation of beams with such a large emittance requires a phase-space painting during injection.

2.2 Ring Design Parameters

Concerning the design of the lattice, the extraction energy was assumed to be 1.5 GeV, rather than 1.0 GeV, which is planned to be the actual extraction energy, because it was expected that the beam energy, if possible, will be upgraded sooner or later to meet the eager requirement for an increase in the beam power. A plan view of the ring is shown in Fig. 2. Since the injection energy is not very high, we don't need a specially long straight section for the charge-exchange injection system, which is proposed in a race-track-type or a triangular-type ring. We thus adopted a conventional highly symmetric lattice, taking into acount the advantage that the density of the structure resonance with a large stop band generally becomes lower in such a lattice. The beam optics are shown in Fig. 3.

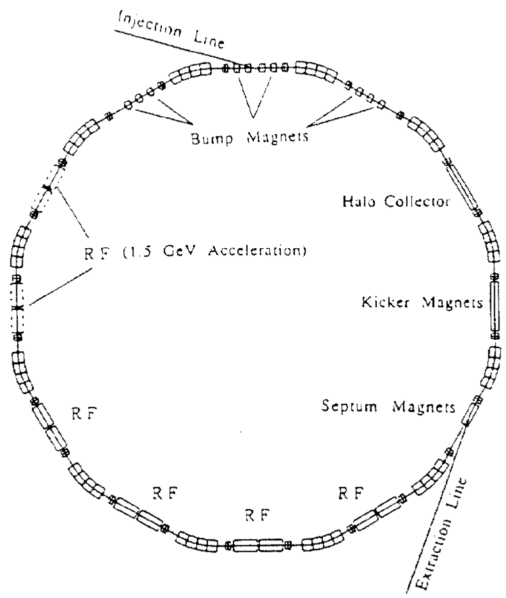

Fig. 2 Plan view of PRIME

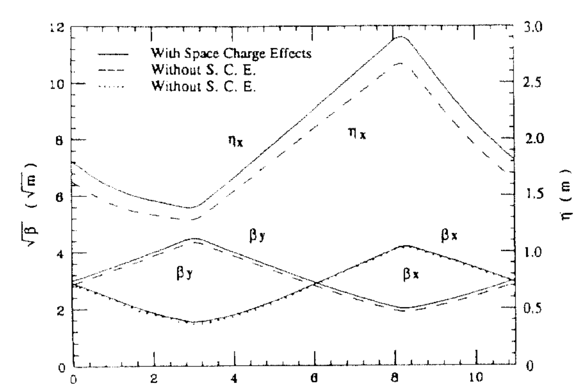

Fig. 3 Beta and dispersion functions of a cell

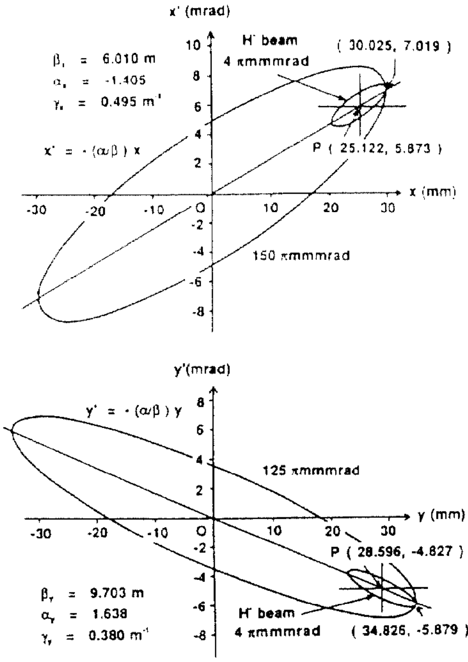

Fig. 4 Emittance ellipses of the injected and ring beam at the injection point

As shown in Fig. 4, the emittance ellipse of the ring beam is much larger than that of the injected H⁻ beam. The ring beam is formed by moving the H⁻ beam between points P and O in the figure. Point O indicates the closed orbit of the ring. It is O that is actually moved, by varying a bump of the closed orbit. We call the variable bump used for painting the "painting bump". The painting bump is shown in Fig. 5. In addition to the painting bump, another orbit bump is necessary to keep the stripping foil outside the ring beam. This bump is shown in Fig. 6, and is called as an "offset bump". The amplitude of the offset bump is fixed during injection.

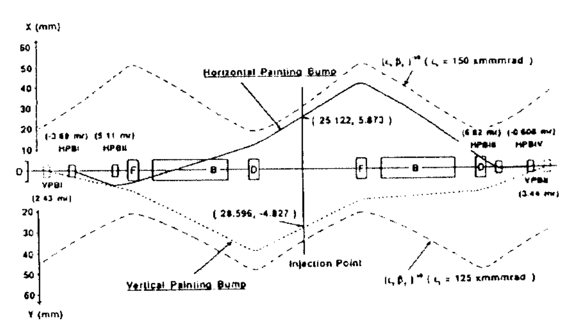

Fig. 5 Arrangement of painting bump magnets and the orbits formed by them

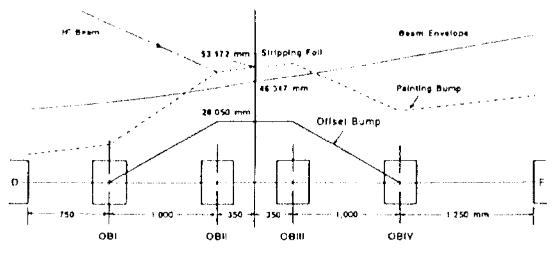

Fig. 6 Offset bump system and the location of the stripping foil for the horizontal plane injection

Table 2 Main parameters of the ring

Lattice and ion optical parameters			
Lattice type		FBDO	
Number of cells		12	
Length of long straight section		4.6	m
Circumference		131.6	m
Betatron oscillation frequency			
	ν_x	3.8	
	ν_y	2.8	
Beta-function	β_x	2.2 ~ 17.4	m
	β_y	3.6 ~ 18.9	m
Dispersion function	η	1.3 ~ 2.7	m
Chromaticity	Horizontal	- 4.3	
	Vertical	- 3.1	
Transition energy		2.36	GeV
Synchrotron magnets and the power supply			
Bending magnet	field strength	0.32 - 1.10	T
	field length	3.57	m
	gap height	120	mm
Focusing Q-mag	field gradient	1.18 - 4.13	T/m
	field length	0.5	m
	bore radius	90	mm
Defocusing Q-mag	field gradient	1.10 - 3.85	T/m
	field length	0.5	m
	bore radius	83	mm
Power supply	50 Hz resonant network		
number of meshes		12	
magnet current	DC	1860	A
	AC	1032	A
choke AC current		516	A
network total DC loss		2670	kW
network total AC loss		610	kW
RF accelerator system			
Acc. cavity	length	~1.75	m
Ferrite	TDK SY-3 (μ_r = 250)		
	diameter	0.512 - 0.250	m
	thickness	25.4	mm
	ferrite number/station	32	
Shunt impedance (Acc. Vol. 15 kV)		~1.4	kΩ
Accelerating voltage/station		15	kV
Number of accelerating cavities		8	
Peak power/station		~300	kVA
Average power/station		~200	kVA

3. SIMULATION OF BEAM PAINTING

The beam-painting method is very crucial because some important characteristics of the beam, such as the emittance growth, are definitely affected by the charge distribution of the beam. Therefore, the resultant charge distribution was examined for some painting methods by a computer simulation code. The code is able to perform tracking along a synchrotron for at most 4,000 macro particles. On simulating the injection process, the tracking continues during 500 turns of circulation around a ring, adding 8 macro particles every turn for the injected particles. Table 3 shows the six methods tested by varying the position of the injected H^- beam.

Table 3 Six injection methods tested

	x (mm)	y (mm)
A	25.1	28.6
B	$25.1\,(t/t_0)$	$28.6\,(t/t_0)$
C	$25.1\,(t/t_0)$	$28.6\,(1 - (t/t_0))$
D	$25.1\,(t/t_0)^{1/2}$	$28.6\,(1 - (t/t_0))^{1/2}$
E	$25.1\,(t/t_0)^{1/2}$	$28.6\,(1 - (t/t_0))$
F	$12.6\,(t/t_0)^{1/2}(1 - \cos 20\pi(t/t_0))$	$28.6\,(1 - (t/t_0))^{1/2}$

t: time delay from injection start (μsec)
t_0: injection period (μsec)

In case A, the resultant beam has an almost square cross section and the particle density becomes high at the four corners. Case B also results in a square cross section, but the particle density becomes high at the center. In case F, the particle density is not uniform to the horizontal direction, but is concentrated at the center. A uniform particle distribution was not obtained by this method. By methods C, D and E, a beam with an elliptic or nearly elliptic shape could be formed; it was also found that these methods were useful to form a beam with a nearly uniform particle distribution. Although the motion of the painting bump is complicated for methods C and D, the beam hitting probabilities at the foil are as low as those for methods A and B.

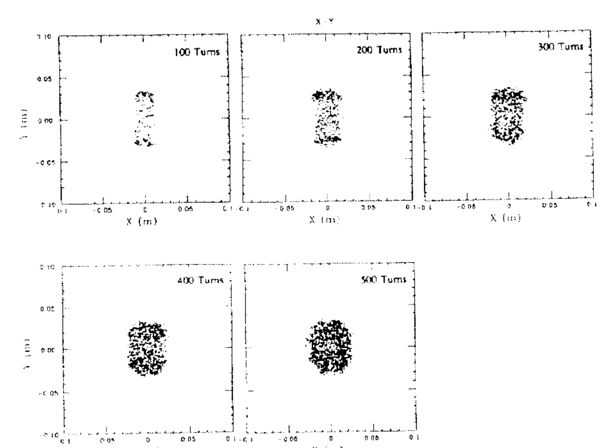

Fig. 7 Evolution of the particle distribution in the real space for the painting method D